PAPER

NJC
www.rsc.org/njc

Preparation, characterization and electrochemical and X-ray structural studies of new conjugated 1,1′-ferrocenediyl-ended [CpFe-arylhydrazone]$^+$ salts

Carolina Manzur,*[a] César Zúñiga,[a] Lorena Millán,[a] Mauricio Fuentealba,[a] Jose A. Mata,[b] Jean-René Hamon*[c] and David Carrillo*[a]

[a] *Laboratorio de Química Inorgánica, Instituto de Química, Pontificia Universidad Católica de Valparaíso, Avenida Brasil, 2950, Valparaíso, Chile. E-mail: david.carrillo@ucv.cl; Fax: +56 32 27 34 20; Tel: +56 32 27 31 65*

[b] *Departamento de Química Inorgánica y Orgánica, Universitat Jaume I, 12080, Casstellón, Spain*

[c] *Laboratoire des Organométalliques et Catalyse: Chimie et Electrochimie Moléculaires CNRS UMR 6509, Institut de Chimie de Rennes, Université de Rennes 1, Campus de Beaulieu, 35042, Rennes cedex, France. E-mail: jean-rene.hamon@univ-rennes1.fr; Fax: +33 223 23 56 37; Tel: +33 223 23 59 58*

Received* (*in Montpellier, France*) *23rd July 2003, Accepted 23rd September 2003
First published as an Advance Article on the web 14th November 2003

A series of new conjugated bimetallic ferrocenyl 1,1′-bis-substituted compounds of the type (*E*)-[CpFe(η^6-*p*-RC_6H_4)NHN=CH(η^5-C_5H_4)Fe(η^5-C_5H_4)–CH=CHC_6H_4-*p*-R′]$^+PF_6^-$ (Cp = η^5-C_5H_5; R, R′ = H, NO_2, **11**; Me, NO_2, **12**; MeO, NO_2, **13**; Cl, NO_2, **14**; Me, CN, **15**; Me, Me, **16**), with end-capped (*E*)-ethenylaryl and [CpFe(arylhydrazone)]$^+$ substituents, have been prepared by the condensation reaction of 1,1′-(*p*-R′-arylethenyl)ferrocenecarboxaldehyde (R′ = Me, **4**; NO_2, **5**; CN, **6**) with the organometallic hydrazine precursors [CpFe(η^6-*p*-$RC_6H_4NHNH_2$)]$^+PF_6^-$ (R = H, **7**; Me, **8**; MeO, **9**; Cl, **10**). In the trimetallic series, {[CpFe(η^6-*p*-RC_6H_4)NHN=CH(η^5-C_5H_4)]$_2$Fe}$^{2+}$[PF_6^-]$_2$ (R = H, **17**; Me, **18**; MeO, **19**, Cl, **20**), which results from the condensation of two equivalents of the same organometallic hydrazine precursor (**7**–**10**) with 1,1′-ferrocenedicarboxaldehyde, the ferrocenediyl core symmetrically links two cationic mixed-sandwich units. These ten hydrazones (**11**–**20**) were stereoselectively obtained as their trans isomers about the N=C double bond. All the new compounds were thoroughly characterized by a combination of elemental analysis, spectroscopic techniques (^{1}H NMR, IR and UV-Vis) and electrochemical studies in order to prove electronic interaction between the donating and accepting units through the π-conjugated system. A representative example of each series has also been characterized by single crystal X-ray diffraction analysis. The bimetallic complex **16**$^+$ adopts an anti conformation with the two iron atoms on opposite faces of the dinucleating hydrazonato ligand, whereas the trinuclear complex **19**$^{2+}$ adopts a syn conformation with an Fe–Fe–Fe angle of 180°. Other salient features of these structures are the long Fe–C_{ipso} bond distances and the slight cyclohexadienyl character at the coordinated C_6 ring, with a folding angle of 7.4° and 7.0° for **16**$^+$ and **19**$^{2+}$, respectively.

Introduction

Ferrocenes[1] play important roles in the fields of organic and organometallic chemistry and in materials science as components of dendrimers,[2] polymers,[3] molecular magnets[4] and non-linear optical (NLO) materials.[5] Their chemistry has been extensively explored because ferrocene-based complexes combine chemical versatility and excellent thermal and photochemical stability with exceptional electrochemical properties, which generate considerable interest in the use of the ferrocenyl moiety, [CpFe(η^5-C_5H_4)] (Cp = η^5-C_5H_5), as a donating group in donor-acceptor (D-π-A) chromophores displaying enhanced second-order NLO properties.[5,6] The electron-releasing ability of the parent ferrocenyl group is closely similar to that of the *p*-methoxyphenyl group.[7] On the other hand, the cationic isolobal electron-acceptor counterparts of ferrocene, the robust mixed-sandwich derivatives [CpFe(η^6-arene)]$^+$, have also been the subject of intense synthetic,[8] electron transfer,[9] electrochemical[10] and photochemical[11] investigations. Despite this interest, only in one case has the [CpFe(η^6-aryl)]$^+$ moiety been used as an organometallic chromophore to achieve second-order NLO responses.[12] In the search for new materials with electronic communication between terminal subunits, we have focused our interest in the preparation of new conjugated ferrocenyl complexes with end-capped mixed-sandwich iron(II) fragments,[13] affording interesting bimetallic complexes in which the organometallic termini are connected by an asymmetric –NR–N=CR– (R = H, Me) type I hydrazonato[14] conjugated bridge. Furthermore, non-linear optical responses can be envisaged from electrochemical studies, electronic spectroscopy, molecular structure determinations and theoretical investigations that suggest effective electron delocalization along the π-conjugated spacer.[13b,d,e]

In a continuation of these studies, we have now prepared conjugated ferrocenyl 1,1′-bis-substituted compounds with end-capped arylethenyl substituents and [CpFe(arylhydrazone)]$^+$ groups for the bimetallic series **11**–**16**, whereas in the trimetallic series **17**–**20**, the ferrocenediyl core symmetrically links two cationic mixed-sandwich units. The full analytical

DOI: 10.1039/b308626g

and spectroscopic characterization (IR, UV-VIS, ^{1}H NMR) of these ten new organometallic hydrazone complexes and of the new 1,1′-(*p*-tolylethenyl)ferrocenecarboxaldehyde (**4**) and its protected 1,3-dioxolane precursor **3** (see below) are reported here. Their electronic and electrochemical properties have been investigated and the crystal structures of a representative example of each series, namely compounds **16** and **19**, have also been determined. Structurally related dicationic trinuclear organoiron oligomers have recently been prepared by Abd-El-Aziz *et al.*[15] in order to synthesize a new class of mixed-charge iron-containing polymers. In addition, 1,1′- bis-ethenediyl ferrocene complexes with various pendant groups such as pyridine,[16] *p*-cyano,[17] *p*-bromo[18] and *p*-iodophenylene[19] have been used by several authors to synthesize trimetallic derivatives that show very interesting structural features and high non-linear optical responses.

Results and discussion

Synthesis and spectroscopy of 3 and 4

As pointed out by most authors, the *E*-type conformation of the π-bridge is known to provide a good coplanarity of the conjugated spacer and hence to increase the electronic communication between the donating and accepting ends of a dipolar system.[17–21] Therefore, we first attempted to prepare the new bis-substituted ferrocene compound (*E*)-1,1′-(*p*-methylstyryl)-ferrocene carboxaldehyde (**4**, Scheme 1) by conventional Wittig methods, the most appropriate strategy for short-length chained complexes, according to the procedure described by Peris and co-workers for the analogous derivatives **5** and **6**, bearing the *p*-nitro and *p*-cyano electron-withdrawing groups, respectively.[17] The reaction afforded a poor yield of an untractable mixture and therefore, in order to obtain our target molecule **4**, we applied the multi-step procedure developped by Manoury *et al.*[21] (Scheme 1). This involves the preparation of the monoacetal **2** from 1,1′-ferrocenedicarboxaldehyde **1**, which is readily accessible from ferrocene.[22] The free aldehyde function was then used to build the first substituent by reacting **2** with the *in situ* generated (*p*-$MeC_6H_4CH{=}PPh_3$) ylide. Surprisingly, compound **3** was stereoselectively formed, in 59% yield, as the *E* isomer as demonstrated by ^{1}H NMR spectroscopy (see below). The Wittig reaction generally leads to a mixture of *E* and *Z* isomers. Hydrolytic deprotection of the 1,3-dioxolane intermediate **3** furnished the desired bis-substituted ferrocene carboxaldehyde **4** in 47% yield (Scheme 1). The new free formyl group has then been used in the building up of the second substituent as described in the following section.

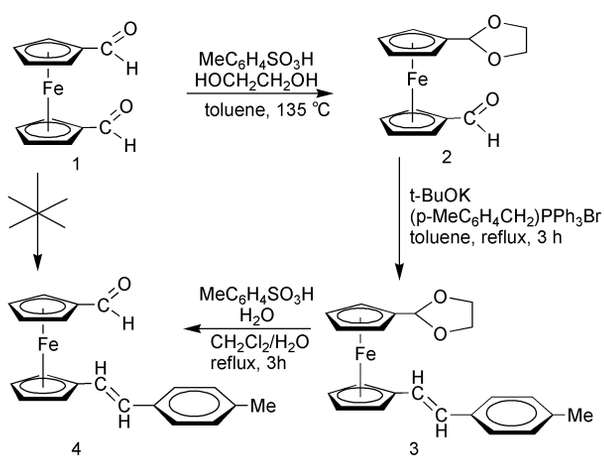

Scheme 1

Characterization of the new products **3** and **4** was mainly achieved by means of IR and ^{1}H NMR spectroscopies and satisfactory elemental analysis (see Experimental). In the proton NMR spectra, both *E* isomers **3** and **4** are identified by their AB quartet with a coupling constant of *ca.* 17 Hz, in accord with the expected *trans* stereochemistry. Four triplets were observed for the substituted Cp rings, while the phenyl protons appear as two doublets. On the other hand, the carboxaldehyde function of compound **4** exhibited the characteristic strong ν(C=O) stretching vibration at 1679 cm^{-1} in the infrared spectrum, and low field singlets at δ 9.91 and δ 192.7 in the ^{1}H and ^{13}C{^{1}H} NMR spectra, respectively.

The cyclovoltammogram of complex **4** displayed the chemically reversible ferrocene/ferricinium couple with $i_{pa}/i_{pc} = 1.0$ in CH_2Cl_2. The large peak-to-peak separation (196 mV) may be due to a combination of uncompensated solution resistance and slightly slow electron transfer kinetics.[23] As expected as the result of substituting an electron-withdrawing group (NO_2, CN) for an electron-releasing one (Me), the half-wave potential of the ferrocenediyl core for **4** (267 mV) is less anodic, with respect to ferrocene, than those measured for **5** (310 mV) and **6** (330 mV),[17] indicating some degree of electron transfer between the *p*-Me substituent and the iron center.

Synthesis and spectroscopy of 11–20

The 1-carboxaldehyde-1′-*p*-R′-(*E*)-styrylferrocenes (η^5-C_5H_4CHO)Fe(η^5-C_5H_4–(*E*)–CH=CH–C_6H_4-*p*-R′) (R′ = Me, **4**; NO_2, **5**; CN, **6**) are indeed of interest in the design of new materials, since the presence of the carboxaldehyde group can provide access to a variety of functional groups. Thus, the new dinuclear organoiron hydrazones **11**–**16** (see Experimental and Table 1) were successfully prepared by a condensation reaction of the ionic organometallic hydrazine precursors [CpFe(η^6-*p*-$RC_6H_4NHNH_2$)]$^+PF_6^-$ (R = H, **7**; Me, **8**; MeO, **9**; Cl, **10**) with the ferrocene-based aldehyde building blocks **4**–**6** (Scheme 2).

On the other hand, the trimetallic hydrazones [{CpFe(η^6-*p*-$RC_6H_4NHN{=}CH$–η^5-C_5H_4)}$_2$Fe]$^{2+}$[PF_6^-]$_2$ (**17**–**20**; see Experimental and Table 2) were synthesized by the reaction of 2 equiv. of organoiron hydrazine precursors **7**–**10** with 1,1′-ferrocenedicarboxaldehyde (η^5-C_5H_4CHO)$_2$Fe (Scheme 3). It is interesting to note that the bis functionalized *p*-chloro derivative **20** represents an attractive monomeric unit for the preparation of polymers containing both neutral and cationic cyclopentadienyliron complexes in their structures, in light of the recently communicated synthetic methodology.[15]

In all cases, the reactions were carried out in refluxing ethanol solution containing catalytic amounts of concentrated acetic acid. The bi- and trinuclear complexes were obtained as spectroscopically pure air- and thermally stable, brownish red to dark red (**11**–**16**) and orange or red-orange (**17**–**20**) microcrystalline solids in reasonable yields ranging from 40 to 59%, after recrystallization from CH_2Cl_2–Et_2O (1:1). The cationic compounds exhibit a good solubility in common polar organic solvents, but are insoluble in diethyl ether, hydrocarbons and water. The structures of these ten new homobi- and homotrimetallic hydrazones were inferred from satisfactory elemental analyses (Table 3), ^{1}H NMR, IR and UV-Vis spectroscopies (Table 4) and, additionally, in the case of complexes **16** and **19**, by X-ray diffraction analysis (*vide infra*).

The most remarkable common features observed in the IR spectra of these ten powdered compounds (**11**–**20** in Table 4) were: (i) the existence of a sharp intense band at *ca.* 1570 cm^{-1}, which is due to the asymmetric stretching vibration of the C=N imine group, (ii) the typical weak to medium N–H stretching vibration in the region from 3316 to 3344 cm^{-1} and (iii) a very strong $\nu(PF_6)$ band at *ca.* 840 cm^{-1} and a sharp and strong δ(P–F) band at 557–559 cm^{-1}. In addition, the

Table 1 Reactions of organoiron hydrazine complexes with *p*-substituted styrylferrocenecarboxaldehydes[a]

Compound	R, R′	$[CpFe(p\text{-}RC_6H_4NHNH_2)]^+PF_6^-$	$(C_5H_4CHO)Fe(C_5H_4–CH=CHC_6H_4\text{-}p\text{-}R'$	Yield
11	H, NO_2	49.8 mg, 0.138 mmol	49.8 mg, 0.138 mmol	55%, 54 mg
12	Me, NO_2	53.6 mg, 0.138 mmol	49.8 mg, 0.138 mmol	58%, 58 mg
13	MeO, NO_2	55.8 mg, 0.138 mmol	49.8 mg, 0.138 mmol	55%, 57 mg
14	Cl, NO_2	56.5 mg, 0.138 mmol	49.8 mg, 0.138 mmol	53%, 55 mg
15	Me, CN	100.0 mg, 0.258 mmol	87.0 mg, 0.255 mmol	40%, 72 mg
16	Me, Me	50.0 mg, 0.129 mmol	43.0 mg, 0.130 mmol	56%, 50 mg

[a] The reactions listed in this table were all run under the general conditions given in the Experimental.

infrared spectra of compounds **11**–**16** showed a weak band in the 1588–1620 cm^{-1} region assigned to the ν(C=C) stretching mode of the phenylethenyl pendant group. More specifically, the IR spectra of compounds **11**–**14** exhibited a strong band in the range 1333–1340 cm^{-1} attributed to the *p*-NO_2 substituent, whereas the C≡N stretching vibration appeared at 2221 cm^{-1} in the IR spectrum of **15**. Finally, the spectra of the homotrimetallic compounds **17** and **20** showed *two* N=C, PF_6^- (and C–Cl for **20**) stretching frequencies (see Table 4), a phenomenon that we have already encountered for homobimetallic ferrocenyl hydrazone complexes, which is compatible with the presence of at least two conformers in the solid state.[13b]

Interestingly, the organoiron hydrazones **11**–**20** are stereoselectively formed as the sterically less hindered trans (about the N=C double bond) isomer as indicated by the unique set of signals in their ^1H NMR spectra (acetone-d_6, 297 K, see Table 4) and definitively assigned from the structural analyses of **16** and **19** (see below). For all the compounds, the two sandwich moieties $[CpFe(\eta^6\text{-}p\text{-}RC_6H_4–)]^+$ and $[(\eta^5\text{-}C_5H_4)_2Fe]$ are clearly identified by the characteristic sharp singlet of the Cp proton resonance observed at *ca.* 5.0 ppm while the two monosubstituted C_5 rings appeared as broad singlets or unresolved triplets in the 4.80–4.86 and 4.53–4.56 ppm ranges, corresponding to the spectrum of an A_2B_2 system. Only one pair of H_α and H_β resonances is observed for the trimetallic compounds **17**–**20**, consistent with a symmetrical structure with an inversion center at the ferrocenediyl iron atom, in agreement with the solid state structure of **19** (see below). The *p*-substituted phenylethenyl pendant groups of the bimetallic derivatives **11**–**16** exhibited the same resonance and coupling constant patterns as those reported above for the ferrocene-based aldehyde **4**, indicating that the trans stereochemistry about the HC=CH double bond is retained after the construction of the hydrazone framework. The low field position (δ 9.26–9.59) of the acidic benzylic N–H[24] signal may be attributed to the electronic effect of the organometallic moiety,[8a,25] and/or its participation in molecular association *via* intermolecular H-bonding.[13d] Finally, the upfield-shifted aromatic protons of the coordinated C_6 ring and the deshielded sharp proton resonance at *ca.* 7.90 ppm assigned to the azomethine fragment (N=CH) appeared in the expected regions.[13]

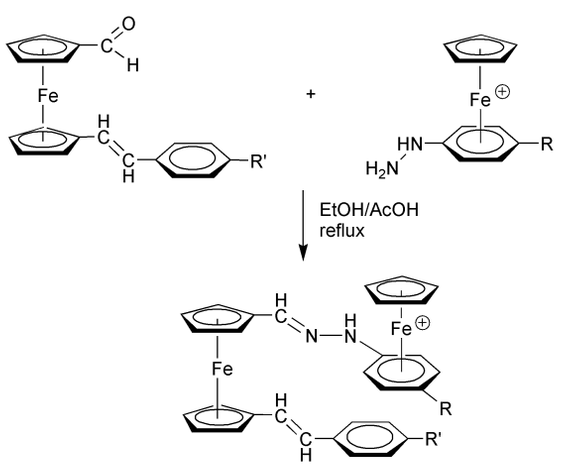

R,R'= H,NO_2 **11**; Me,NO_2 **12**; MeO, NO_2 **13**; Cl, NO_2 **14**; Me, CN **15**, Me, Me **16**

Scheme 2

Crystal structures

The molecular structures of the cationic (*E*)-$[CpFe(\eta^6\text{-}p\text{-}MeC_6H_4)–NHN=CH–(\eta^5\text{-}C_5H_4)Fe(\eta^5\text{-}C_5H_4)–CH=CH–C_6H_4\text{-}p\text{-}Me]^+$ (**16**$^+$) and of the dicationic $[\{CpFe(\eta^6\text{-}p\text{-}MeOC_6H_4)–NHN=CH–(\eta^5\text{-}C_5H_4)\}_2Fe]^{2+}$ (**19**$^{2+}$) organometallic moieties, along with the atom labelling schemes, are presented in Fig. 1 and Fig. 2, respectively. Key bond lengths and angles for **16**$^+$ and **19**$^{2+}$ are listed in Table 5. In both complexes, high anisotropic thermal motion and/or disorder was observed for the carbon atoms of the Cp ligand of the mixed-sandwich units. Such a phenomenon has frequently been reported for mixed-sandwich iron(II) complexes.[13b, 13c, 24, 26, 27] The orientation is presumably due to partial rotation of the C_5 ring about the Fe–Cp centroid axis. The metrical parameters (see Table 5) are typical of η^5–Fe–η^6 and η^5–Fe–η^5 metallocene-type coordination.[28–31] The carbocyclic rings coordinated to the same iron center are essentially parallel with one another and the ring centroid–iron–ring centroid vectors are almost collinear, both in the $[Cp–Fe–arene]^+$ and in the ferrocenic subunits.

Complex **16**$^+$ adopts an *anti* conformation[13b] with the two iron atoms on opposite faces of the dinucleating hydrazonato ligand (Fig. 1), whereas the trinuclear complex **19**$^{2+}$ adopts a *syn* conformation[13b] with an Fe(1)–Fe(2)–Fe(1a) angle of 180° (Fig. 2). Both $[CpFe(arene)]^+$ moieties occupy opposite sites and they are related by symmetry through the inversion center of the molecule. In both complexes, the π-conjugated bridging ligands, $[p\text{-}RC_6H_4–NHN=CH–C_5H_4]^-$ (R = Me, **16**$^+$; MeO, **19**$^{2+}$), are similar and, therefore, the through-bond Fe···Fe distances (9.714 and 9.633 Å, respectively) are closely related, whereas the through-space Fe···Fe distance is much longer in **16**$^+$ (8.064 Å) than in **19**$^{2+}$ (6.925 Å). In complex **16**$^+$ the ferrocenylidene groups adopt an eclipsed conformation whereas the staggered one is observed for complex **19**$^{2+}$ (see Figs. 1 and 2). The conformation adopted by the dinuclear complex **16**$^+$ allows a certain interaction between the coordinated and free phenyl groups, although the dihedral angle between them is 41.65° (see Fig. 1). On the other hand, the coordinated and non-coordinated phenyl groups are not coplanar with the corresponding Cp and Cp′ ligands of the ferrocenylidene group, subtending dihedral angles of 21.31° and 18.96°, respectively. The phenyl group of the trimetallic species is not coplanar with the Cp ligand, subtending a dihedral angle of 27.70° (see Fig. 2). These significant but not large deviations from planarity might, however, allow an efficient π-electron delocalization or electronic interaction between the electron-donating and electron-accepting termini through the entire hydrazonato skeleton.

Table 2 Reactions of organoiron hydrazine complexes with 1,1′-ferrocenedicarboxaldehyde[a]

Compound	R	$[CpFe(p\text{-}RC_6H_4NHNH_2)]^+PF_6^-$	$(C_5H_4CHO)_2Fe$	Yield
17	H	101.0 mg, 0.270 mmol	32.0 mg, 0.132 mmol	55%, 69 mg
18	Me	109.5 mg, 0.282 mmol	34.0 mg, 0.140 mmol	51%, 70 mg
19	MeO	115.1 mg, 0.285 mmol	34.6 mg, 0.143 mmol	50%, 73 mg
20	Cl	51.5 mg, 0.126 mmol	15.0 mg, 0.062 mmol	59%, 37 mg

[a] The reactions listed in this table were all run under the general conditions given in the Experimental.

A careful examination of Table 5 reveals some interesting structural features provoked by the strong electron-withdrawing effect of $CpFe^+$ on the arene ligand in both complexes. Thus, the Fe(1)–C(6) bond lengths, 2.193(5) and 2.144(4) Å for $\mathbf{16}^+$ and $\mathbf{19}^{2+}$, respectively, are longer than the mean value of the other Fe(1)–C(C_6 ring) bond lengths (see Table 5). Such an Fe–C elongation has already been reported by us for the binuclear organometallic hydrazones.[13b,13c] This remarkable elongation is a consequence of a partial delocalization of the electron pair located on the N(1) atom toward the mixed-sandwich moiety and is reflected by (i) a depyramidalization of the N(1) atom with typical bond angles of an sp^2-hybridized nitrogen atom (Table 5), (ii) a C(6)–N(1) bond length of 1.359(6) Å for $\mathbf{16}^+$ and 1.366(4) Å for $\mathbf{19}^{2+}$, values that are intermediate between those of a single and a double carbon–nitrogen bond[31] and (iii) a slight cyclohexadienyl-like character at the coordinated phenyl ring with a folding angle of 7.4° and 7.0° about the C(7)–C(11) axis for both complexes, respectively. Likewise, the Fe(1)–C(9) bond length of 2.116(5) Å in complex $\mathbf{19}^{2+}$ can be also attributed to a partial delocalization of one oxygen lone pair toward the arene ligand, provoking a folding angle around the C(8)–C(10) axis of 5.8°. Hence, the arene ligand adopt a slightly bowed conformation, with the C(6) and C(9) atoms being bent out of the carbocyclic diene plane.

Electronic spectra

Electronic absorption spectra for the cationic bi- and trinuclear hydrazones **11**–**20** were measured in CH_2Cl_2 and DMSO; the values are recorded in Table 4. In each solvent the complexes exhibited similar spectra, revealing their isostructural features with two sets of absorption maxima typical of conjugated ferrocenyl systems. The lower energy band (400–500 nm) is assigned to a metal-to-ligand charge-transfer transition (MLCT) and the higher lying absorption in the range of 300 to 360 nm as an intraligand π-π* transition (ILCT). In fact, both bands have some d-d character.[32–34] These assignments are in agreement with previously reported theoretical[35] and experimental data.[17,19–21,36,37] The energy and intensity of these transitions are influenced by the nature of the ancillary ligands, giving rise to bathochromic shifts in its absorption maximum as the result of a lowering of the energy of the π* orbital of the ligand.[5a,37a] The effect can be further amplified by increasing the acceptor strength of the electron deficient center. Examination of the UV-vis data (Table 4) for the series of four compounds containing the same $[(\eta^5\text{-}C_5H_4)Fe(\eta^5\text{-}C_5H_4)\text{–}CH{=}N\text{–}NH\text{–}(\eta^6\text{-}p\text{-}MeC_6H_4)FeCp]^+PF_6^-$ framework and bearing various pendant accepting groups, such as (p-CH=CH–$C_6H_4NO_2$) (**12**), (p-CH=CH–C_6H_4CN) (**15**), (p-CH=CH–C_6H_4Me) (**16**) and $[CpFe^+(\eta^6\text{-}p\text{-}MeC_6H_4\text{-}NHN{=}CH)]$ (**18**), indicates that the energies and the oscillator strengths of both the low and high energy bands are sensitive to the acceptor strength. Thus, while compound **16** exhibits λ_{max} at 302 and 453 nm, these values progressively shift to longer wavelengths in going to **18** (309 and 473 nm), **15** (311 and 478 nm) and finally to **12** (321 and 492 nm). Similar trends are observed for other families of ferrocenyl p-cyanophenylethenyl and phenylethynyl compounds,[36c,38] as well as for cationic organoiron polymers containing azo-dye-functionalized side chains.[39]

The two characteristic CT bands of the dinuclear hydrazones **11**–**13**, **15** and **16** exhibit bathochromic shifts (Fig. 3) on changing from CH_2Cl_2 ($\varepsilon = 8.90$) to DMSO ($\varepsilon = 47.6$), indicating increased polarity in the excited state. The more intense π-π* band is more solvatochromic (4–22 nm) than the lower energy band. For the dinuclear hydrazone **14** and the trinuclear compounds **17**–**20**, the higher energy band is also red-shifted (6–22 nm) but the lower energy band shows a negative solvatochromism (−2 to −55 nm, see Fig. 3). This results from a better stabilization of the equilibrium ground state than the Franck–Condon excited state, due to solvation by solvents of increasing polarity.[40] Such a negative solvatochromism (hypsochromic shift) is mainly observed for cationic derivatives,[13b,13d,37] since in these species the ground state dipole moments are opposite in sign to those of the neutral species,[41] due to the acceptor-localized positive charges, but the charge transfer is in the same direction as in the neutral species.

It is worth noting that the lower energy maxima for the dicationic ferrocenediyl hydrazones **17**–**20** are found to be somewhat blue-shifted compared to those of the neutral bis-substituted ferrocenediyl-ligated phenylethenyl derivatives, $Fe\{(\eta^5\text{-}C_5H_4)\text{-}(E)\text{-}CH{=}CHC_6H_4\text{-}p\text{-}R\}_2$ (R = NO_2, CN), reported by Peris *et al.*[17] Coordination of the arene rings with two [$CpFe^+$] fragments is expected to generate stronger dicationic electron-accepting termini. The half-wave oxidation potentials of trimetallic hydrazone derivatives are indeed slightly more anodic than those of the mononuclear neutral species. A rather similar situation has been pointed out by Heck and co-workers[37b] and two factors were argued to explain this apparent inconsistency: (i) the generation of new orbital frontiers, with changes in character and order, upon complexation and (ii) the molecular orbitals involved in the oxidation step and in the photochemical excitation can be different.

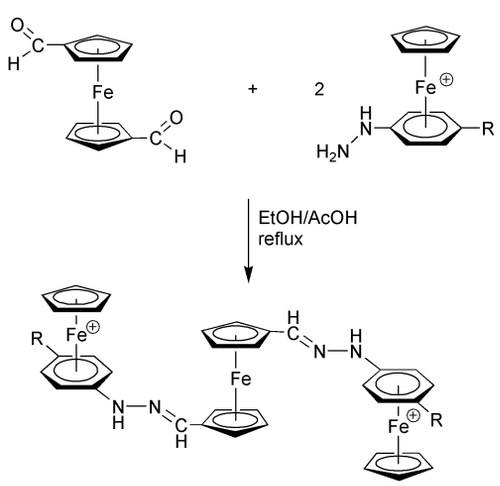

R= H **17**; Me **18**; MeO **19**; Cl **20**

Scheme 3

Table 3 Some properties of the new bi- and trimetallic hydrazone complexes

Compound	Color	M. p.[a]/°C	Analyses
11	Brownish red	149	Found: C, 49.88; H, 3.87; N, 5.76 Calcd.: C, 50.24; H, 3.65; N, 5.86
12	Brownish red	105	Found: C, 51.12; H, 4.00; N, 5.67 Calcd.: C, 50.92; H, 3.86; N, 5.75
13	Brownish red	97	Found: C, 50.29; H, 3.89; N, 5.94 Calcd.: C, 49.83; H, 3.78; N, 5.62
14	Brownish red	187	Found: C, 48.24; H, 3.56; N, 5.98 Calcd.: C, 47.94; H, 3.35; N, 5.59
15	Dark red	155	Found: C, 53.79; H, 4.12; N, 6.33 Calcd.: C, 54.04; H, 3.97; N, 5.91
16	Dark red	215	Found: C, 55.25; H, 4.61; N, 4.09 Calcd.: C, 54.89; H, 4.46; N, 4.00
17	Orange	209	Found: C, 43.13; H, 3.40; N, 6.06 Calcd.: C, 42.80; H, 3.38; N, 5.87
18	Orange	263	Found: C,43.78; H, 3.78; N, 5.92 Calcd.: C, 44.02; H, 3.69; N, 5.70
19	Orange	240	Found: C, 42.80; H, 3.64; N, 5.79 Calcd.: C, 42.64; H, 3.58; N, 5.52
20	Red-orange	215	Found: C, 40.32; H, 3.17; N, 5.39 Calcd.: C, 39.92; H, 2.96; N, 5.48

[a] All the compounds decompose when melted.

Electrochemical studies

In order to get a deeper insight into the mutual donor-acceptor electronic influence with respect to electrochemical perturbations, we have undertaken the cyclic voltammetry (CV) study of the homobi- and homotrimetallic hydrazone complexes (**11**–**16** and **17**–**20**, respectively). All the cyclovoltammograms were recorded in DMF using the same setup and the electrochemical data thus obtained are summarized in Table 6. All the complexes display two major features: (i) an irreversible process attributable to Fe-centered reduction at the mixed-sandwich fragment[10,33b] and (ii) a single chemically reversible oxidation wave corresponding to the ferrocenyl unit[42] in the bridging linker (Fig. 4). As for the ferrocenediyl-based aldehyde precursor **4**, the peak-to-peak separations (ΔE_p, see Table 6) are significantly greater than the ideal value of 59 mV required for a pure Nernstian process, probably due to the same reasons cited above.[23] However, this difference is similar to that measured for ferrocene under the conditions of the experiment (see Experimental for details).

By comparison with the previously reported monocationic series, $[CpFe(\eta^6\text{-}p\text{-}RC_6H_4)NHN{=}CH(\eta^5\text{-}C_5H_4)FeCp]^+$,[13b,43] the bis-substituted complexes show a greater anodic shift (*ca.* 20–100 mV) of their half-wave potentials, except for **16** as expected with its donating *p*-Me group and, more surprisingly, **18** (see Table 6). This suggests that the extra electron-accepting substituent has a significant electronic effect on the ferrocenyl bridging spacer. Also surprising is the more anodic half-wave potential of the nitrile derivative **15** compared to that of the corresponding nitro counterpart **12**, despite the known better electron-accepting nature of the nitro group. This was already noted for the precursor aldehydes **5** and **6**.[17] The substitution of the arylethenyl groups by the corresponding organometallic hydrazone ligands, **13** *vs.* **19**, **14** *vs.* **20**, **16** *vs.* **18**, results in a shift of the oxidation wave to more anodic potential, presumably due to the powerful electron-accepting nature of the cationic mixed-sandwich unit.

On the reduction side, the ten compounds studied undergo an irreversible process (Fig. 4) centered at the mixed-sandwich moiety, corresponding to the single-electron reduction of the d^6, Fe(II), 18-electron complexes to the unstable d^7, Fe(I), 19-electron species.[10,33b] The very cathodic potential values (Table 6) are very similar to those reported for the monometallic benzaldehyde hydrazone[24] and homobimetallic elongated hydrazone-linker-containing complexes[13e] and are presumably due to the reduction of an *in situ* generated neutral zwitterionic species.[24,44] As expected for the symmetric homotrimetallic compounds **17**–**20**, the integrated area of the reduction wave is twice that of the oxidation one. Note that the cyclovoltammogram of **20** exhibits two reduction waves at −2.30 and −2.44 V *vs.* $Cp_2Fe^{0/+}$, the more anodic one being attributable to a dechlorination reaction.[45,46]

On the other hand, the cyclovoltammograms of the four appended *p*-NO_2 substituent derivatives **11**–**14** exhibit two fully reversible reduction waves at *ca.* −1.32 and −1.53 V *vs.* $Cp_2Fe^{0/+}$. The first wave is confidently assigned to the monoelectronic reduction of the nitro group to generate the radical anion $-NO_2^{\bullet -}$,[47,48] whereas the assignment of the second reversible wave remains much more puzzling.[49] Nevertheless, this indicates that the LUMO for complexes **11**–**14** is localized at the nitro substituent. For compounds **15**–**20**, however, the LUMO is determined by the cationic mixed-sandwich, and in all the cases, the nature of the HOMO is dominated by the neutral donating ferrocenyl units, in accordance with theoretical investigations.[13b] All these electrochemical data taken together suggest that the electron-donating and -accepting termini communicate electronically to a significant extent and that they behave as a donor-acceptor couple.

Concluding remarks

In conclusion, we have described the easy access to two new homogeneous series of conjugated ferrocenyl 1,1′-bis-substituted compounds with end-capped arylethenyl substituents and $[CpFe(arylhydrazone)]^+$ groups for the bimetallic series **11**–**16** whereas in the trimetallic series **17**–**20**, the ferrocenediyl core symmetrically links two cationic mixed-sandwich units, *via* condensation reactions between cyclopentadienyliron-complexed hydrazines and ferrocene mono- and biscarbaldehydes, respectively. Single crystal X-ray diffraction analyses show that the bimetallic complex $\mathbf{16}^+$ adopts an *anti* conformation with the two iron atoms on opposite faces of the dinucleating hydrazonato ligand, whereas the trinuclear complex $\mathbf{19}^{2+}$ adopts a *syn* conformation with a linear Fe–Fe–Fe arrangement. The ten new organometallic hydrazones **11**–**20** can be defined as type I non-rod-shaped dipolar chromophores.[14] The cationic mixed-sandwich $[CpFe(\eta^6\text{-}p\text{-}RC_6H_4)\text{–}]^+$ acts as an electron acceptor and the neutral ferrocenediyl moiety as an electron-donating group. Their mutual electronic influence is mediated by the hydrazone linking spacer –NH–N=CH–. Moreover, depending on the nature of their *p*-substituents, the arylethenyl pendent groups act either as electron-withdrawing (*p*-NO_2, *p*-CN) or -releasing (*p*-Me) entities. We have shown that these respective electronic properties clearly influence the values of the redox potential in the cyclovoltammograms and the energies of the charge transfer bands in the electronic spectra. As a result, these compounds are proved to favour electronic delocalization along the conjugated chain. Finally, the polarized structure of this type of complexes, which endows them with solvatochromic properties, suggests that they are good candidates for non-linear optical studies. Further work will now be directed toward the determination of those properties for some selected dipolar organometallic hydrazone complexes reported here.

Experimental

General methods and materials

All operations were performed under inert atmosphere using standard vacuum/nitrogen line, Schlenk or syringe techniques with protection from light to avoid decomplexation of the $CpFe^+$ moiety. The solvents were dried and distilled under

Table 4 Spectroscopic data of the new bi- and trimetallic iron hydrazone complexes

Compound	IR (KBr) ν/cm^{-1}	UV-vis λ/nm (Log ε/dm^3 mol^{-1} cm^{-1})	^{1}H NMR[a] δ (CD_3COCD_3)
11	3328 m (NH), 1590 m (C=C), 1570 m (C=N), 1333 s (NO_2), 840 vs and 558 m (PF_6)	CH_2Cl_2: 322 (4.40), 489 (3.71) DMSO: 332 (4.33), 488 (3.62)	4.55 (br s, 4H, C_5H_4), 4.81 (br s, 2H, C_5H_4), 4.86 (br s, 2H, C_5H_4), 5.03 (s, 5H, Cp), 6.10–6.21 (m, 5H, coord Ph), 6.88 (d, $J_{H\text{-}H}$ = 16.3, 1H, CH=CH), 7.16 (d, $J_{H\text{-}H}$ = 16.2, 1H, CH=CH), 7.60 (d, $J_{H\text{-}H}$ = 8.8, 2H, Ph), 7.88 (s, 1H, N=CH), 8.00 (d, $J_{H\text{-}H}$ = 8.9, 2H, Ph), 9.42 (br s, 1H, NH)
12	3328 m (NH), 1588 m (C=C), 1570 m (C=N), 1338 s (NO_2), 840 vs and 557 m (PF_6)	CH_2Cl_2: 321 (4.36), 351sh (4.32), 492 (3.67) DMSO: 327 (4.33), 341sh (4.32), 501 (3.62)	2.46 (s, 3H, CH_3), 4.53 (br s, 4H, C_5H_4), 4.80 (t, $J_{H\text{-}H}$ = 1.7, 2H, C_5H_4), 4.83 (t, $J_{H\text{-}H}$ = 1.7, 2H, C_5H_4), 4.96 (s, 5H, Cp), 6.05–6.08 (m, 4H, coord Ph), 6.87 (d, $J_{H\text{-}H}$ = 16.2, 1H, CH=CH), 7.15 (d, $J_{H\text{-}H}$ = 16.2, 1H, CH=CH), 7.60 (d, $J_{H\text{-}H}$ = 8.8, 2H, Ph), 7.88 (s, 1H, N=CH), 7.98 (d, $J_{H\text{-}H}$ = 8.9, 2H, Ph), 9.43 (br s, 1H, NH)
13	3330 m (NH), 1590 m (C=C), 1570 m (C=N), 1337 s (NO_2), 1256 s (C–O), 840 vs and 557 m (PF_6)	CH_2Cl_2: 315 (4.31), 357sh (4.25), 487 (3.64) DMSO: 332 (4.35), 351 (4.32), 490 (3.69)	4.02 (s, 3H, CH_3O), 4.53 (br s, 4H, C_5H_4), 4.80 (t, $J_{H\text{-}H}$ = 1.7, 2H, C_5H_4), 4.83 (t, $J_{H\text{-}H}$ = 1.7, 2H, C_5H_4), 5.00 (s, 5H, Cp), 6.00 (d, $J_{H\text{-}H}$ = 6.9, 2H, coord Ph), 6.12 (d, $J_{H\text{-}H}$ = 6.9, 2H, coord Ph), 6.88 (d, $J_{H\text{-}H}$ = 16.2, 1H, CH=CH), 7.15 (d, $J_{H\text{-}H}$ = 16.1, 1H, CH=CH), 7.61 (d, $J_{H\text{-}H}$ = 8.7, 2H, Ph), 7.86 (s, 1H, N=CH), 8.01 (d, $J_{H\text{-}H}$ = 8.7, 2H, Ph), 9.36 (br s, 1H, NH)
14	3324 m (NH), 1590 m (C=C), 1558 m (C=N), 1340 s (NO_2), 1098 w (C–Cl), 836 vs and 556 s (PF_6)	CH_2Cl_2: 323 (4.44), 355 (4.39), 487 (3.79) DMSO: 331 (4.38), 462 (3.71)	4.53 (t, $J_{H\text{-}H}$ = 1.7, 2H, C_5H_4), 4.56 (t, $J_{H\text{-}H}$ = 1.7, 2H, C_5H_4), 4.81 (t, $J_{H\text{-}H}$ = 1.7, 2H, C_5H_4), 4.85 (t, $J_{H\text{-}H}$ = 1.7, 2H, C_5H_4), 5.12 (s, 5H, Cp), 6.18 (d, $J_{H\text{-}H}$ = 6.8, 2H, coord Ph), 6.53 (d, $J_{H\text{-}H}$ = 6.6, 2H, coord Ph), 6.87 (d, $J_{H\text{-}H}$ = 16.2, 1H, CH=CH), 7.14 (d, $J_{H\text{-}H}$ = 16.3, 1H, CH=CH), 7.60 (d, $J_{H\text{-}H}$ = 8.7, 2H, Ph), 7.89 (s, 1H, N=CH), 8.01 (d, $J_{H\text{-}H}$ = 8.8, 2H, Ph), 9.59 (br s, 1H, NH)
15	3331 w (NH), 2221 m (C≡N), 1620 w (C=C), 1572 m (C=N), 838 vs and 557 s (PF_6)	CH_2Cl_2: 250 (4.26), 286 (3.96), 311 (4.04), 343 (4.12), 407 (3.33), 478 (3.27) DMSO: 316 (4.24), 353 (4.11), 428 (3.17), 479 (3.26)	2.47 (s, 3H, CH_3), 4.49 (m, 4H, C_5H_4), 4.78 (m, 4H, C_5H_4), 4.91 (s, 5H, Cp), 6.00 (d, $J_{H\text{-}H}$ = 5.2, 2H, coord Ph), 6.09 (d, $J_{H\text{-}H}$ = 5.3, 2H, coord Ph), 6.74 (d, $J_{H\text{-}H}$ = 16.4, 1H, CH=CH), 7.00 (d, $J_{H\text{-}H}$ = 16.2, 1H, CH=CH), 7.46 (s, 4H, Ph), 7.80 (s, 1H, N=CH), 9.30 (br s, 1H, NH)
16	3331 w (NH), 1620 w (C=C), 1572 m (C=N), 838 vs and 557 s (PF_6)	CH_2Cl_2: 274 (4.03), 302 (3.15), 327 (3.45), 360 (3.08), 453 (3.04) DMSO: 261 (4.38), 308 (3.93), 331 (4.32), 418 (3.13), 465 (3.49)	2.34 (s, 3H, CH_3), 2.52 (s, 3H, CH_3), 4.55 (br s, 4H, C_5H_4), 4.84 (br s, 4H, C_5H_4), 4.99 (s, 5H, Cp), 6.08 (d, $J_{H\text{-}H}$ = 6.2, 2H, coord Ph), 6.17 (d, $J_{H\text{-}H}$ = 6.3, 2H, coord Ph), 6.60 (d, $J_{H\text{-}H}$ = 16.0, 1H, CH=CH), 6.77 (d, $J_{H\text{-}H}$ = 16.1, 1H, CH=CH), 7.02 (d, $J_{H\text{-}H}$ = 7.9, 2H, Ph), 7.23 (d, $J_{H\text{-}H}$ = 7.8, 2H, Ph), 7.86 (s, 1H, N=CH), 9.26 (br s, 1H, NH)
17	3316 w (NH), 1570 s and 1560 s (C=N), 842 vs, 831 vs and 558 m (PF_6)	CH_2Cl_2: 240(3.95), 277(3.30), 312(3.85), 351(3.45), 410(3.09), 491 (2.92) DMSO: 319 (3.84), 356 (3.59), 419 (3.15), 466 (3.05)	4.54 (br s, 4H, C_5H_4), 4.85 (br s, 4H, C_5H_4), 5.01 (s, 10H, Cp), 6.06–6.51 (m, 10H, Ph), 8.00 (s, 2H, N=CH), 9.54 (s, 2H, NH)
18	3336 m (NH), 1568 s (C=N), 844 vs, 826 vs and 558 s (PF_6)	CH_2Cl_2: 239 (4.15), 274 (3.40), 309 (3.98), 349 (3.71), 407 (3.16), 473 (3.13) DMSO: 272 (3.47), 315 (3.46), 355 (3.34), 407 (2.62), 457 (2.76)	2.44 (s, 6H,CH_3), 4.54 (br s, 4H, C_5H_4), 4.85 (br s, 4H, C_5H_4), 4.94 (s, 10H,Cp), 6.10 (br s, 8H, Ph), 7.83 (s, 2H, N=CH), 9.23 (s, 2H, NH)
19	3344 m (NH), 1570 s (C=N), 1252 s (C–O), 841 vs and 558 s (PF_6)	CH_2Cl_2: 242 (3.88), 274 (3.78), 313 (3.80), 354 (3.61), 404 (3.00), 470 (2.99) DMSO: 270 (3.80), 319 (3.61), 360 (3.46), 417 (3.16), 468 (3.01)	3.98 (s, 6H, CH_3O), 4.53 (br s, 4H, C_5H_4), 4.83 (br s, 4H, C_5H_4), 4.98 (s, 10H,Cp), 6.03 (d, $J_{H\text{-}H}$ = 6.9, 4H, Ph), 6.11 (d, $J_{H\text{-}H}$ = 7.1, 4H, Ph), 7.79 (s, 2H, N=CH), 9.17 (s, 2H, NH)
20	3329 m (NH), 1570 s and 1560 s (C=N), 1092 w and 1062 w (C–Cl), 843 vs, 829 vs and 557 s (PF_6)	CH_2Cl_2: 240 (3.86), 290 (2.88), 302 (3.59), 345 (3.56), 416 (2.91), 487 (2.89) DMSO: 274 (3.81), 324 (3.79), 359 (3.43), 433 (3.13)	4.54 (br s, 4H, C_5H_4), 4.85 (br s, 4H, C_5H_4), 5.10 (s, 10H, Cp), 6.23 (br s, 4H, Ph), 6.53 (br s, 4H, Ph), 7.83 (s, 2H, N=CH), 9.49 (s, 2H, NH)

[a] Recorded at 200 MHz for **11**–**16** and at 400 MHz for **17**–**20**.

nitrogen by standard methods prior to use. Microanalytical data were obtained by the Institut de Chimie de Rennes Microanalysis Service on a Thermo-Finigan Flash EA 1112 CHNS analyser. IR spectra were obtained with a Perkin Elmer Model 1600 FT-IR spectrophotometer. Electronic spectra were recorded in CH_2Cl_2 and DMSO solutions with a Spectronic Genesys 2 spectrophotometer. All the ^{1}H NMR spectra were recorded in acetone-d_6, unless otherwise stated, on multinuclear Bruker DPX 200 and Avance 400 Digital NMR Bruker spectrometers at 297 K; all chemical shifts are reported in parts per million (ppm) relative to internal tetramethylsilane (Me_4Si), with the residual solvent proton resonance as internal standards. Coupling constants are given in Hertz (Hz).

Electrochemical measurements were performed using a Radiometer Analytical model PGZ 100 All-in-One potentiostat, using a standard three-electrode setup with a vitreous

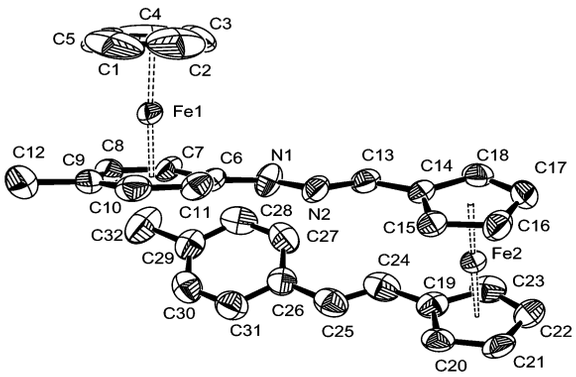

Fig. 1 Molecular structure and atom numbering scheme for the cation (*E*)-[CpFe(η^6-*p*-MeC_6H_4)–NHN=CH–(η^5-C_5H_4)Fe(η^5-C_5H_4)–CH=CH–C_6H_4-*p*-Me]$^+$ (**16**$^+$). Hydrogen atoms and counter anion PF_6^- have been omitted for clarity. Displacement ellipsoids are at the 50% probability level.

carbon (in DMF) or Pt (in CH_2Cl_2) working electrode, platinum wire auxiliary electrode and Ag/AgCl as the reference electrode. DMF and CH_2Cl_2 solutions were 1.0 mM of the compound under study and 0.1 M of the supporting electrolyte *n*-$Bu_4N^+PF_6^-$. The $Cp_2Fe^{0/+}$ couple, located at 0.560 and 0.445 V under those conditions in DMF and CH_2Cl_2, respectively, was used as an internal reference for the potential measurements. $E_{\frac{1}{2}}$ is defined as equal to $(E_{pa} + E_{pc})/2$, where E_{pa} and E_{pc} are the anodic and cathodic peak potentials, respectively.

Chromatography columns (typically *ca.* 20 cm in length and *ca.* 2 cm in diameter) were packed with silica gel (Aldrich, 60 Å). Melting points were determined in evacuated capillaries and were not corrected.

The 4-(*p*-R-benzyl)triphenylphosphonium bromides (R = NO_2, CN, Me) were prepared by a procedure similar to that described in ref. 50. 2-(1′-Formylferrocenyl)-1,3-dioxolane (**2**),[21] 1-formyl-1′-(*E*)-(*p*-nitrostyryl)ferrocene (**5**)[17] and the hydrazine complexes [CpFe(η^6-*p*-RC_6H_4NHNH_2)]$^+PF_6^-$ (R = H, **7**; Me, **8** and MeO, **9**;[26a] R = Cl, **10**[13b]) were prepared according to published procedures. 1-Formyl-1′-(*E*)-(*p*-cyanostyryl)ferrocene (**6**)[17] was directly obtained as the desired pure *E* isomer using the protected/deprotected 1,3-dioxolane route described in ref. 21. Other chemicals were purchased from commercial sources and used as received.

Syntheses

1,1′-Ferrocenedicarboxaldehyde (1)[22b]. Compound **1** was prepared according to literature procedure, using the same quantities of reagents, with the following modifications to the work-up. After the organic phase was dried over $MgSO_4$, the title compound was purified by column chromatography on silica gel washed beforehand with hexane. First, the use of hexane as eluant produced the release of an orange band that allowed to collect unreacted ferrocene. The deep purple band eluted afterwards with a hexane –CH_2Cl_2 (1:1) mixture was discarded, and finally elution with pure CH_2Cl_2 produced the release of the desired red band, which was collected. The solvent was removed under reduced pressure and the product was dried *in vacuo*, yielding 3.80 g (15.7 mmol, 60%) of **1** as a shiny red microcrystalline powder, authentified by comparison of its ^{1}H NMR parameters with those reported in the original article.[22b]

(*E*)-2-[1′-(4-Methylstyryl)ferrocenyl]-1,3-dioxolane (3). Potassium *tert*-butoxide (667 mg, 5.94 mmol) was mixed with 2.29 g (5.13 mmol) of 4-(*p*-methylbenzyl)triphenylphosphonium bromide in 20 cm^3 of dry toluene and refluxed for 3 h under N_2. After cooling to room temperature, a solution of 551 mg (1.93 mmol) of 2-(1′-formylferrocenyl)-1,3-dioxolane (**2**), dissolved in 15 cm^3 of dry toluene, was added and the solution was warmed again to reflux for 3 h. After cooling back to room temperature, the solution was concentrated to 5 cm^3 and then absorbed on a column containing silica gel and eluted with a pentane–diethyl ether mixture (1:2 v/v) to produce the release of an orange band, which was collected and concentrated to dryness on a rotary evaporator. The orange microcrystalline powder of **3** was collected and dried *in vacuo*. Yield: 422 mg (1.13 mmol, 59%). M.p. 115 °C. Anal. calcd for $C_{22}H_{22}FeO_2$ (%): C, 70.60; H, 5.93; found: C, 70.75; H, 5.73. ^{1}H NMR (400 MHz, CD_3COCD_3) δ: 2.32 (s, 3H, CH_3), 3.86–4.01 (m, 4H, CH_2–CH_2), 4.41 (t, 2H, C_5H_4, J_{H-H} = 1.8 Hz), 4.66 (t, 2H, C_5H_4, J_{H-H} = 1.8 Hz), 4.67 (t, 2H, C_5H_4, J_{H-H} = 1.8 Hz), 4.79 (t, 2H, C_5H_4, J_{H-H} = 1.8 Hz), 5.68 (s, 1H, O–CH–O), 6.78 (d, 1H, CH=CH, J_{H-H} = 17 Hz), 6.93 (d, 1H, CH=CH, J_{H-H} = 16 Hz), 7.16 (d, 2H, Ph, J_{H-H} = 7.3 Hz), 7.39 (d, 2H, Ph, J_{H-H} = 7.7 Hz). IR (KBr pellets) ν_{max}/cm^{-1}: 3087w, 3014vw (CH), 2957w, 2917vw, 2841w, 2753vw (CH), 1664m (C=C), 1091s, 1029s (C–O).

(*E*)-1′-(4-Methylstyryl)ferrocenecarboxaldehyde (4). To a solution of 505 mg (1.35 mmol) of **3** in 15 cm^3 of dichloromethane was added 50 mg (0.263 mmol) of *p*-toluenesulfonic acid monohydrate in 5 cm^3 of deoxygenated water, then the mixture was refluxed for 3 h under N_2. After cooling to room temperature, the organic phase was separated, dried over $MgSO_4$ and concentrated to 3 cm^3, absorbed on a column containing silica gel and eluted with a pentane–diethyl ether mixture (1:2 v/v) to produce the release of a red-orange band, which was collected and concentrated to dryness on a rotary evaporator. The red-orange microcrystalline powder of **4** was collected and dried *in vacuo*. Yield: 208 mg (0.63 mmol, 47%). M.p. 96 °C. Anal. calcd for $C_{20}H_{18}FeO$ (%): C, 72.75;

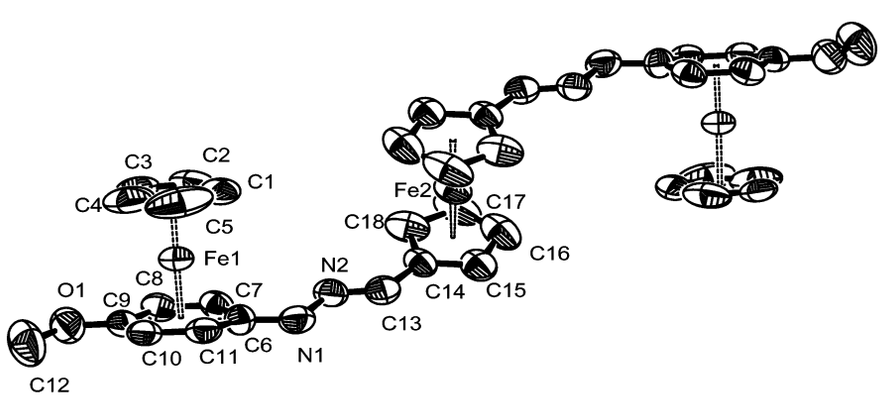

Fig. 2 Molecular structure and atom numbering scheme for the dication [{CpFe(η^6-*p*-MeOC_6H_4)–NHN=CH–(η^5-C_5H_4)}$_2$Fe]$^{2+}$ (**19**$^{2+}$). Hydrogen atoms and counter anion PF_6^- have been omitted for clarity. Displacement ellipsoids are at the 50% probability level.

Table 5 Selected bond lengths (Å) and bond angles (deg.) for cations $\mathbf{16}^+$ and $\mathbf{19}^+$.[a] Standard deviations are given in parentheses

	$\mathbf{16}^+$	$\mathbf{19}^+$		**16**	**19**
C–C(1–5)[b]	1.308	1.346	C–C(6–11)[b]	1.406	1.392
C(9)–O(1)	–	1.360(5)	C(6)–N(1)	1.359(6)	1.366(4)
N(1)–N(2)	1.383(5)	1.382(4)	N(2)–C(13)	1.278(6)	1.275(4)
C(13)–C(14)	1.448(7)	1.421(5)	C–C(14–18)[b]	1.415	1.411
C–C(19–23)[b]	1.412	–	C(19)–C(24)	1.455(8)	–
C(24)–C(25)	1.296(7)	–	C(25)–C(26)	1.501(8)	–
Fe(1)–C(1–5)[b]	2.011	2.045	Fe(1)–C(6)	2.193(5)	2.144(4)
Fe(1)–C(7)	2.087(5)	2.073(4)	Fe(1)–C(8)	2.064(5)	2.048(4)
Fe(1)–C(9)	2.084(5)	2.116(5)	Fe(1)–C(10)	2.056(5)	2.077(4)
Fe(1)–C(11)	2.098(5)	2.064(4)	Fe(2)–C(14–18)[b]	2.050	2.039
Fe(2)–C(19–23)[b]	2.048	–	Fe(1)···Fe(2)[c]	9.714	9.633
Fe(1)···Fe(2)[d]	8.064	6.925	Fe(1)–Cp_{CNT}	1.675	1.658
Fe(1)–Ph_{CNT}	1.565	1.556	Fe(2)–Cp_{CNT}	1.658	1.649
Fe(2)–Cp'_{CNT}	1.659	–			
C(6)–N(1)–N(2)	120.7(4)	120.5(4)	N(1)–N(2)–C(13)	114.9(4)	117.2(4)
N(2)–C(13)–C(14)	121.2(5)	123.2(5)	C(19)–C(24)–C(25)	127.5(6)	–
C(24)–C(25)–C(26)	126.5(6)	–	Cp_{CNT}–Fe(1)–Ph_{CNT}	179.0	179.2
Cp'_{CNT}–Fe(2)–Cp_{CNT}	178.9	–			

[a] Abbreviations: Cp = η^5-C_5H_5, Cp′ = η^5-C_5H_4, Ph = η^6-C_6H_4, CNT = centroid. [b] Average distance. [c] Sum of the bond distances. [d] Measured through-space distance.

H, 5.49; found: C, 72.97; H, 5.56. ^{1}H NMR (400 MHz, CD_3COCD_3) δ: 2.32 (s, 3H, CH_3), 4.41 (t, 2H, C_5H_4, J_{H-H} = 1.8 Hz), 4.62 (t, 2H, C_5H_4, J_{H-H} = 1.8 Hz), 4.67 (t, 2H, C_5H_4, J_{H-H} = 1.8 Hz), 4.78 (t, 2H, C_5H_4, J_{H-H} = 1.8 Hz), 6.82 (d, 1H, CH=CH, J_{H-H} = 17 Hz), 6.87 (d, 1H, CH=CH, J_{H-H} = 17 Hz), 7.17 (d, 2H, Ph, J_{H-H} = 8.1 Hz), 7.40 (d, 2H, Ph, J_{H-H} = 8.1 Hz), 9.91 (s, 1H, CHO). $^{13}C\{^1H\}$ NMR (100 MHz, $CDCl_3$) δ: 20.3 (CH_3), 67.9 (C_5H_4), 70.2 (C_5H_4), 70.3 (C_5H_4), 73.9 (C_5H_4), 80.5 (q-C_5H_4), 85.7 (q-C_5H_4), 124.2 (CH=CH), 126.0 (Ph), 127.7 (CH=CH), 129.2 (Ph), 135.0 (q-Ph), 136.8 (q-Ph), 192.7 (CHO). IR (KBr pellets) ν_{max}/cm^{-1}: 3090w, 3078w, 3045vw, 3022vw (CH), 2924vw, 2889w, 2856vw (CH), 1679s (HC=O), 1663m (C=C). UV-vis (CH_2Cl_2) λ_{max}/nm (Log ε/dm^3 mol^{-1} cm^{-1}): 263 (4.25), 318 (4.33), 366 (3.38), 464 (3.13); (DMSO): 264 (4.28), 320 (4.41), 374 (3.19), 474 (3.08). CV $E_{1/2}$/V *vs.* Ag/AgCl (ΔE_p/mV), v = 0.1 V s^{-1}: DMF (working electrode: vitreous carbon) 0.813 (119); CH_2Cl_2 (working electrode: Pt) 0.737 (196).

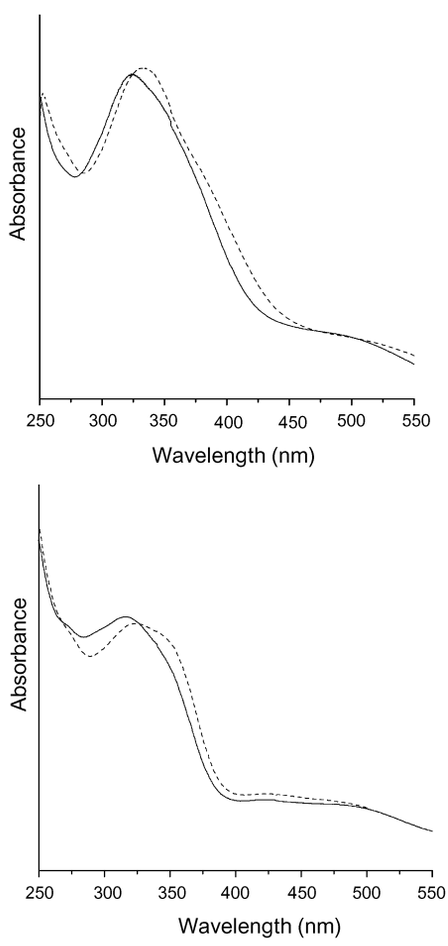

Fig. 3 Electronic spectra of **12** (left) and **20** (right), recorded in CH_2Cl_2 (full line) and in DMSO (dashed line).

Bimetallic hydrazones complexes 11–16. General procedure. A mixture of the indicated quantities (see Table 1 for reagents, stoichiometries and yields) of the solid [CpFe(η^6-*p*-$RC_6H_4NHNH_2$)]$^+PF_6^-$ (R = H, **7**; Me, **8**; MeO, **9**; Cl, **10**) and 1-formyl-1′-(*E*)-(*p*-R′-styryl)ferrocene (R′ = Me, **4**, NO_2, **5**; CN, **6**) was dissolved in 5 cm^3 ethanol containing 5 drops of concentrated acetic acid. The solution was refluxed for 5 h, allowed to stand at room temperature and then at −30 °C overnight (12 h). The precipitate was filtered off, washed first with cold EtOH and then with 5 cm^3 of diethyl ether, then dried under vacuum. Crystallization from saturated dichloromethane solutions by slow diffusion of diethyl ether at room temperature provided the products as crystalline solids. Color, melting point and elemental analyses of the new hydrazone compounds **11**–**16** so prepared are given in Table 3. IR, UV-vis and ^{1}H NMR data are gathered in Table 4.

Trimetallic hydrazone complexes 17–20. General procedure. To a suspension of the indicated quantities (see Table 2 for reagents, stoichiometries and yields) of solid hydrazine precursors **7**–**10** in 5 cm^3 of EtOH was added 0.5 equiv. of 1,1′-ferrocenedicarboxaldehyde (**1**); the reaction mixture was refluxed for 3–5 h. After cooling to room temperature, 1 cm^3 of diethyl ether was added to the orange solution, which was then stored at −30 °C overnight (12 h). The precipitate was filtered off and dissolved in 2 cm^3 of dichloromethane. The solution was filtered through Celite and the filtrate was concentrated to half of its volume, then layered with an equivalent amount of diethyl ether to yield the products as crystalline solids. Color,

Table 6 Cyclic voltammetry data[a]

Compound	$E^{\frac{1}{2}}[(C_5H_4)_2Fe]$/V ($\Delta E_p$/mV)	$E_{pc}[CpFe^+$ (aryl)][b] /V	$E^{\frac{1}{2}}(p\text{-}C_6H_4NO_2)$[c] / V ($\Delta E_p$/mV)
11	0.176 (98)	−2.25	−1.36 (131)
			−1.53 (70)
12	0.161 (92)	−2.31	−1.32 (72)
			−1.53 (70)
13	0.167 (90)	−2.30	−1.30 (100)
			−1.53 (60)
14	0.197 (109)	−2.31	−1.31 (72)
			−1.51 (70)
15	0.221 (93)	−2.27	–
16	0.045 (102)	−2.53	–
17	0.093 (71)	−2.59	–
18	0.077 (84)	−2.52	–
19	0.190 (83)	−2.48	–
20	0.225 (90)	−2.30	–
		−2.44	

[a] Recorded in DMF at 298 K with a vitreous carbon working electrode, 0.1 M n-$Bu_4^+PF_6^-$ as supporting electrolyte, scan rate 100 mV s^{-1}. All potentials are quoted in V *vs.* the $Cp_2Fe^{0/+}$ couple used as internal reference. [b] Irreversible wave corresponding to the Fe(II)/Fe(I) couple. [c] Reversible waves corresponding to the reduction of the nitrophenyl pendant group.

melting point and elemental analyses of the new hydrazone compounds **17**–**20** so prepared are given in Table 3. IR, UV-vis and ^{1}H NMR data are gathered in Table 4.

X-Ray Crystallography

Single crystals of (*E*)-[CpFe(η^6-*p*-MeC_6H_4)–NHN=CH–(η^5-C_5H_4)Fe(η^5-C_5H_4)–CH=CH–C_6H_4-*p*-Me]$^+PF_6^-$ (**16**) and of [{CpFe(η^6-*p*-$MeOC_6H_4$)–NHN=CH–(η^5-C_5H_4)}$_2$Fe]$^{2+}$(PF_6^-)$_2$ (**19**) were obtained by slow diffusion of diethyl ether into the corresponding concentrated CH_2Cl_2 solutions of complexes **16** and **19** at room temperature.

A single crystal of complex **16** was mounted on a glass fiber in a random orientation. Data collection was performed at room temperature on a Siemens Smart CCD diffractometer using graphite-monochromated Mo-Kα radiation (λ = 0.71073 Å), using 0.3° of separation between frames and 30 s per frame. Space group assignments are based on systematic absences, E statistics and successful refinement of the structure. The structure was solved by direct methods with the aid of successful difference Fourier maps and was refined using the SHELXTL 5.1 software package.[51] All non-hydrogen were refined anisotropically. Hydrogen atoms were assigned to ideal positions and refined using a riding model. The diffraction frames were integrated using the SAINT[52] package and corrected for absorption with SADABS.[53]

In the case of complex **19**, the data collection was made on a Bruker SMART APEX diffractometer, using 0.3° of separation between frames and 10 s per frame. The structure was solved and refined using SHELXS97[54] and SHELXL97,[54] respectively, both included in the WinGX[55] software package.

The final *R* indices as well as further details concerning the resolution and refinement of the crystal structures of **16** and **19** are presented in Table 7.†

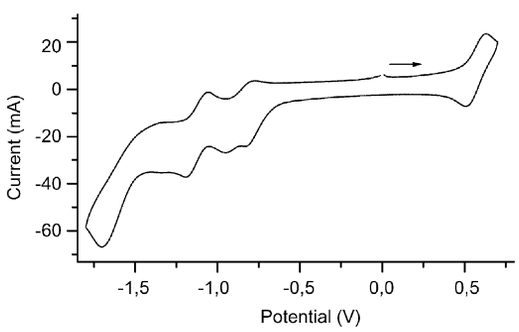

Fig. 4 Cyclic voltammograms of complex **12** recorded in DMF + 0.1 M n-$Bu_4N^+PF_6^-$ at T = 293 K and with a voltage sweep rate v = 0.1 V s^{-1}, reference electrode Ag/AgCl, internal reference $Cp_2Fe^{0/+}$.

Table 7 Crystal data and structure refinement for complexes **16** and **19**

	16	**19**
Empirical formula	$C_{32}H_{31}F_6Fe_2N_2P$	$C_{18}H_{18}F_6Fe_{1.5}N_2OP$
FW/g mol^{-1}	700.26	507.09
T/K	293(2)	293(2)
Crystal system	Triclinic	Orthorhombic
Space group	*P*-1	*Pbca*
a/Å	10.612(3)	12.5730(11)
b/Å	11.147(3)	16.5448(14)
c/Å	13.521(4)	19.0521(16)
α/°	85.155(7)	90
β/°	74.476(7)	90
γ/°	77.999(7)	90
U/Å^3	1506.8(8)	3963.2(6)
Z	2	8
μ/mm^{-1}	1.079	1.260
λ(Mo Kα)/Å	0.71073	0.71073
No. total reflect.	8369	27 421
No. unique reflect.	5129	4559
R_{int}	0.0332	0.0944
R_1 [$I > 2\sigma(I)$]	0.0651	0.0442
wR_2 [$I > 2\sigma(I)$]	0.1192	0.0951
R_1 (all data)	0.0949	0.1291
wR_2 (all data)	0.1271	0.0991

Acknowledgements

We thank Dr. Andrés Vega (Santiago de Chile) for helpful assistance in the structure determination of **19**. We greatly appreciate financial support for this work from the Fondo Nacional de Desarrollo Científico y Tecnológico, FONDECYT (Chile), Grant N° 1010318 (D. C., C. M.), to the Programme International de Coopération Scientifique N° 922 CNRS (France)–CONICYT (Chile and the CNRS-CONICYT Project N° 14531) (C. M., D. C., J.-R. H.), and to the Vicerrectoría de Investigación y Estudios Avanzados, Pontificia Universidad Católica de Valparaíso, Valparaíso, Chile.

References

1 *Ferrocenes: Homogenous Catalysis, Organic Synthesis, Materials Science*, eds. A. Togni and T. Hayashi, Wiley-VCH, Weinheim, 1995.
2 (*a*) D. Astruc, *Pure Appl. Chem.*, 2003, **75**, 461; (*b*) D. Astruc, J.-C. Blais, M.-C. Daniel, V. Martinez, S. Nlate and J. Ruiz, *Macromol. Symp.*, 2003, **196**, 1; (*c*) B. Alonso, E. Alonso, D. Astruc, J.-C. Blais, L. Djakovitch, J.-L. Fillaut, S. Nlate, F. Moulines, S. Rigaut, J. Ruiz and C. Valerio, *Adv. Dendritic Macromol.*, 2002, **5**, 89.
3 (*a*) R. D. A. Hudson, *J. Organomet. Chem.*, 2001, **637–639**, 47; (*b*) P. Nguyen, P. Gómez-Elipe and I. Manners, *Chem. Rev.*, 1999, **99**,

† CCDC reference numbers 188753 for **16** and 209331 for **19**. See http://www.rsc.org/suppdata/nj/b3/b308626g/ for crystallographic data in .cif or other electronic format.

1515; (*c*) A. S. Abd-El-Aziz, *Macromol. Rapid Commun.*, 2002, **23**, 995.
4 J. S. Miller and A. J. Epstein, in *Research Frontiers in Magnetochemistry*, ed. C. J. O'Connor, World Scientific, Singapore, 1993, pp. 283–302 and references therein.
5 (*a*) S. Barlow and S. R. Marder, *Chem. Commun.*, 2000, 1555; (*b*) H. S. Nalwa, *Appl. Organomet. Chem.*, 1991, **5**, 349.
6 For an overview, see: (*a*) S. Di Bella, *Chem. Soc. Rev.*, 2001, **30**, 355; (*b*) J. Heck, S. Dabek, T. Meyer-Friedrichsen and H. Wong, *Coord. Chem. Rev.*, 1999, **190–192**, 1217; (*c*) I. R. Whittall, A. M. McDonagh, M. G. Humphrey and M. Samoc, *Adv. Organomet. Chem.*, 1998, **42**, 291; (*d*) N. J. Long, *Angew. Chem., Int. Ed. Engl.*, 1995, **34**, 21; (*e*) D. R. Kanis, M. A. Ratner and T. J. Marks, *Chem. Rev.*, 1994, **94**, 195.
7 A. N. Nesmeyanov, E. G. Perevalova, S. P. Gubin, K. I. Granberg and A. G. Kozlovsky, *Tetrahedron Lett.*, 1966, **7**, 2381.
8 (*a*) D. Astruc, S. Nlate and J. Ruiz, in *Modern Arene Chemistry*, ed. D. Astruc, Wiley-VCH, Weinheim, 2002, ch. 12, pp. 400–434; (*b*) A. S. Abd-El-Aziz and S. Bernardin, *Coord. Chem. Rev.*, 2000, **203**, 219; (*c*) D. Astruc, *Top. Curr. Chem.*, 1991, **160**, 47; (*d*) D. Astruc, *Tetrahedron*, 1983, **39**, 4027.
9 D. Astruc, *Acc. Chem. Res.*, 1997, **30**, 383.
10 D. Astruc, *Chem. Rev.*, 1988, **88**, 1189.
11 (*a*) W. A. Hendrickson and M. C. Palazzotto, *Photosensitive Metal-Organic Systems*, eds. C. Kutal and N. Serpone, Advanced Chemistry Series 238, American Chemical Society, Washington, DC, 1993, pp. 411–432; (*b*) D. R. Chrisope, K. M. Park and G. B. Schuster, *J. Am. Chem. Soc.*, 1989, **111**, 6195; (*c*) D. R. Chrisope and G. B. Schuster, *Organometallics*, 1989, **8**, 2737.
12 C. Lambert, W. Gaschler, M. Zabel, R. Matschiner and R. Wortmann, *J. Organomet. Chem.*, 1999, **592**, 109.
13 (*a*) C. Manzur, L. Millán, M. Fuentealba, J.-R. Hamon and D. Carrillo, *Tetrahedron Lett.*, 2000, **41**, 3615; (*b*) C. Manzur, M. Fuentealba, L. Millán, F. Gajardo, D. Carrillo, J. A. Mata, S. Sinbandhit, P. Hamon, J.-R. Hamon, S. Kahlal and J.-Y. Saillard, *New J. Chem.*, 2002, **26**, 213; (*c*) C. Manzur, M. Fuentealba, D. Carrillo, D. Boys and J.-R. Hamon, *Bol. Soc. Chil. Quim.*, 2001, **46**, 409; (*d*) C. Manzur, M. Fuentealba, L. Millán, F. Gajardo, M. T. Garland, R. Baggio, J. A. Mata, J.-R. Hamon and D. Carrillo, *J. Organomet. Chem.*, 2002, **660**, 71; (*e*) A. Trujillo, M. Fuentealba, C. Manzur, D. Carrillo and J.-R. Hamon, *J. Organomet. Chem.*, 2003, **681**, 150.
14 (*a*) C. Serbutoviez, C. Bosshard, G. Knöpfle, P. Weiss, P. Prêtre, P. Günter, K. Schenk, E. Solari and G. Chapuis, *Chem. Mater.*, 1995, **7**, 1198; (*b*) M. S. Wong, U. Meier, F. Pan, V. Gramlich, C. Bosshard and P. Günter, *Adv. Mater.*, 1996, **8**, 416.
15 (*a*) A. S. Abd-El-Aziz, E. K. Todd, R. M. Okasha and T. E. Wood, *Macromol. Rapid Commun.*, 2002, **23**, 743; (*b*) A. S. Abd-El-Aziz, E. K. Todd and R. M. Okasha, *Macromol. Symp.*, 2003, **196**, 77.
16 O. Briel, K. Sünkel, I. Krossing, H. Noth, E. Schmalzlin, K. Meerholz, C. Brauchle and W. Beck, *Eur. J. Inorg. Chem.*, 1999, 483.
17 J. A. Mata, E. Peris, R. Llusar, S. Uriel, M. P. Cifuentes, M. G. Humphrey, M. Samoc and B. Luther-Davies, *Eur. J. Inorg. Chem.*, 2001, 2113.
18 J. A. Mata and E. Peris, *Inorg. Chim. Acta*, 2003, **343**, 175.
19 S. K. Hurst, M. G. Humphrey, J. P. Morrall, M. P. Cifuentes, M. Samoc, B. Luther-Davies, G. A. Heath and A. C. Willis, *J. Organomet. Chem.*, 2003, **670**, 56.
20 (*a*) J. C. Calabrese, L.-T. Cheng, J. C. Green, S. R. Marder and W. Tam, *J. Am. Chem. Soc.*, 1991, **113**, 7227; (*b*) H. E. Bunting, M. L. H. Green, S. R. Marder, M. E. Thompson, D. Bloor, P. V. Kolinsky and R. J. Jones, *Polyhedron*, 1992, **11**, 1489.
21 J. Chiffre, F. Averseng, G. G. A. Balavoine, J.-C. Daran, G. Iftime, P. G. Lacroix, E. Manoury and K. Nakatani, *Eur. J. Inorg. Chem.*, 2001, 2221.
22 (*a*) Modifications in the work -up of 1,1′-ferrocenedicarboxaldehyde[22b] have been carried out; see Experimental section for details; (*b*) G. G. A. Balavoine, G. Doisneau and T. Fillebeen-Khan, *J. Organomet. Chem.*, 1991, **412**, 381.
23 D. Astruc, *Electron Transfer and Radical Reactions in Transition-Metal Chemistry*, VCH, New York, 1995, ch. 2, pp. 89–195.
24 C. Manzur, L. Millán, W. Figueroa, D. Boys, J.-R. Hamon and D. Carrillo, *Organometallics*, 2003, **22**, 153.
25 H. A. Trujillo, C. M. Casado, J. Ruiz and D. Astruc, *J. Am. Chem. Soc.*, 1999, **121**, 5674.
26 (*a*) C. Manzur, E. Baeza, L. Millán, M. Fuentealba, P. Hamon, J.-R. Hamon, D. Boys and D. Carrillo, *J. Organomet. Chem.*, 2000, **608**, 126; (*b*) W. Figueroa, M. Fuentealba, C. Manzur, D. Carrillo, J. A. Mata and J.-R. Hamon, *J. Chil. Chim. Soc.*, 2003, **48**, 75.
27 (*a*) S. Marcen, M. V. Jiménez, I. T. Dobrinovich, F. J. Lahoz, L. A. Oro, J. Ruiz and D. Astruc, *Organometallics*, 2002, **21**, 326; (*b*) Y. Ishii, M. Kawaguchi, Y. Ishino, T. Aoki and M. Hidai, *Organometallics*, 1994, **13**, 5062; (*c*) S. Subramanian, L. Wang and M. J. Zaworotko, *Organometallics*, 1993, **12**, 310; (*d*) J.-L. Fillaut, R. Boese and D. Astruc, *Synlett*, 1992, 55; (*e*) K. A. Abboud, S. H. Simonsen, A. Piorko and R. G. Sutherland, *Acta Crystallogr., Sect. C*, 1991, **47**, 860.
28 For exemples of X-ray crystal structures of $[CpFe(\eta^6\text{-arene})]^+$ complexes, see: (*a*) J.-R. Hamon, J.-Y. Saillard, A. Le Beuze, M. J. McGlinchey and D. Astruc, *J. Am. Chem. Soc.*, 1982, **104**, 7549; (*b*) See also refs 11, 13b–d, 24, 26, 27 and 29.
29 P. J. Dyson, M. C. Grossel, N. Shrinivasan, T. Vine, T. Welton, D. J. Williams, A. J. P. White and T. Zigras, *J. Chem. Soc., Dalton Trans.*, 1997, 3465.
30 For structurally characterized bis-substituted ferrocene-based π-bridged systems, see, for example, refs 16–21.
31 For a reference gathering a large number of interatomic and metal-ligand distances obtained from the Cambridge Crystallographic Data Base Centre, see: A. G. Orpen, L. Brammer, F. H. Allen, D. Kennard, D. G. Watson and R. Taylor, *J. Chem. Soc., Dalton Trans.*, 1989, S1.
32 The deconvolution of the lower energy absorption band gave rise to a splitting into two independent bands whose λ_{max} are observed in the 479–483 nm range. We also expect d-d transitions, due to both the cationic mixed sandwich (ref. 33) and the ferrocenyl unit (ref. 34), to be present in the visible part of the spectrum. However, we expect these to be very weak compared to the two charge transfer transitions.
33 (*a*) W. H. Morrison, E. Y. Ho and D. N. Hendrickson, *Inorg. Chem.*, 1975, **14**, 500; (*b*) J.-R. Hamon, D. Astruc and P. Michaud, *J. Am. Chem. Soc.*, 1981, **103**, 758.
34 (*a*) Y. S. Sohn, D. N. Hendrickson and H. B. Gray, *J. Am. Chem. Soc.*, 1971, **93**, 3603; (*b*) Y. Yamaguchi and C. Kutal, *Inorg. Chem.*, 1999, **38**, 4861.
35 S. Barlow, H. E. Bunting, C. Ringham, J. C. Green, G. U. Bublitz, S. G. J. Boxer, J. W. Perry and S. R. Marder, *J. Am. Chem. Soc.*, 1999, **121**, 3715.
36 For neutral chromophores see, for example: (*a*) J. Mata, S. Uriel, E. Peris, R. Llusar, S. Houbrechts and A. Persoons, *J. Organomet. Chem.*, 1998, **562**, 197; (*b*) G. G. A. Balavoine, J.-C. Daran, G. Iftime, P. G. Lacroix, E. Manoury, J. A. Delaire, I. Maltey-Fanton, K. Nakatani and S. Di Bella, *Organometallics*, 1999, **18**, 21; (*c*) J. A. Mata, E. Falomir, R. Llusar and E. Peris, *J. Organomet. Chem.*, 2000, **616**, 80; (*d*) J. A. Mata, S. Uriel, R. Llusar and E. Peris, *Organometallics*, 2000, **19**, 3797; (*e*) J. A. Mata, E. Peris, I. Asselberghs, R. Van-Boxel and A. Persoons, *New J. Chem.*, 2001, **25**, 299; (*f*) I. Janowska, J. Zakrzewski, K. Nakatani, J. A. Delaire, M. Palusiak, M. Walak and H. Scholl, *J. Organomet. Chem.*, 2003, **675**, 35.
37 For cationic chromophores see, for example: (*a*) V. Alain, A. Fort, M. Barzoukas, C.-T. Chen, M. Blanchard-Desce, S. R. Marder and J. W. Perry, *Inorg. Chim. Acta*, 1996, **242**, 43; (*b*) T. Farrell, T. Meyer-Friedrichsen, M. Malessa, D. Haase, W. Saak, I. Asselberghs, K. Wostyn, K. Clays, A. Persoons, J. Heck and A. R. Manning, *J. Chem. Soc., Dalton Trans.*, 2001, 29; (*c*) H. Wong, T. Meyer-Friedrichsen, T. Farrell, C. Mecker and J. Heck, *Eur. J. Inorg. Chem.*, 2000, 631; (*d*) B. J. Coe, L. A. Jones, J. A. Harris, B. S. Brunschwig, I. Asselberghs, K. Clays and A. Persoons, *J. Am. Chem. Soc.*, 2003, **125**, 862.
38 R. P. Hsung, C. E. D. Chidsey and L. R. Sita, *Organometallics*, 1995, **14**, 4808.
39 (*a*) A. S. Abd-El-Aziz, T. H. Afifi, W. R. Budakowski, K. J. Friesen and E. K. Todd, *Macromolecules*, 2002, **35**, 8929; (*b*) A. S. Abd-El-Aziz, E. K. Todd, R. M. Okasha and T. H. Afifi, *Macromol. Symp.*, 2003, **196**, 89.
40 (*a*) C. Reichardt, *Solvents and Solvent Effects in Organic Chemistry*, 2nd edn., VCH, Wenheim, 1988; (*b*) C. Reichardt, *Chem. Rev.*, 1994, **94**, 2319 and references therein.
41 A hypsochromic shift has also been reported for unusual neutral chromophores: P. D. Beer and H. Sikanyika, *Polyhedron*, 1990, **9**, 1091.
42 P. Zanello, in *Ferrocenes: Homogenous Catalysis, Organic Synthesis, Materials Science*, eds. A. Togni and T. Hayashi, Wiley-VCH, Weinheim, 1995, ch. 7, pp. 317–430.
43 The redox potentials of compounds **11**–**20** and those of their counterparts prepared in ref. 13*b* are compared relative to the ferrocene/ferricinium couple used in both cases as internal reference.

44 The benzylic N–H group is indeed strongly activated by both the electron-withdrawing organometallic moiety $CpFe^{+}$ and the imine functionality. Therefore, the thermally stable zwitterion $[CpFe^{+}(p\text{-}RC_6H_4)N^{-}\text{–}N{=}CH(C_5H_4)Fe(C_5H_4R')]$ can be easily formed by deprotonation in the electrochemical medium. No attempts were made to characterize their corresponding non-deprotonated precursors **11**–**20** by CV.

45 This fully irreversible wave could indeed be attributed to the 2-electron reduction of the C–Cl functionality, following the ECE mechanism for the reduction of Ar–X into $Ar^{\bullet}$ and X^{-} (ref. 46). Its integrated area is twice that of the wave at −2.44 V.

46 D. G. Peters, in *Organic Electrochemistry*, eds. H. Lund and O. Hammerich, 4th edn., Marcel Dekker, New York, 2001, ch. 8, pp. 341–377.

47 B. S. Jensen and V. D. Parker, *J. Chem. Soc., Chem. Commun.*, 1974, 367.

48 H. Lund, in *Organic Electrochemistry*, eds. H. Lund and O. Hammerich, 4th edn., Marcel Dekker, New York, 2001, ch. 9, pp. 379–409.

49 For detailed mechanistic investigations on the reduction of nitroaromatic compounds see: (*a*) A. Darchen and C. Moinet, *J. Electroanal. Chem.*, 1976, **68**, 173; (*b*) A. Darchen and C. Moinet, *J. Chem. Soc., Chem. Commun.*, 1976, 820; (*c*) A. Darchen and C. Moinet, *J. Electroanal. Chem.*, 1977, **81**, 78.

50 R. Ketcham, D. Jambotkar and L. Martinelli, *J. Org. Chem.*, 1962, **27**, 4666.

51 G. M. Sheldrick, *SHELXTL, version 5.1*, Bruker AXS, Inc., Madison, WI, USA, 1997.

52 *SAINT, version 5.0*, Bruker Analytical X-Ray Systems, Madison, WI, USA, 1998.

53 G. M. Sheldrick, *SADABS Empirical Absorption Program*, University of Göttingen, Göttingen, Germany, 1996.

54 G. M. Sheldrick, *SHELXS-97, Program for solution of crystal structures (release 97-2)*, University of Göttingen, Germany, 1997; G. M. Sheldrick, *SHELXL-97, Program for refinement of crystal structures (release 97-2)*, University of Göttingen, Germany, 1997.

55 L. J. Farrugia, *J. Appl. Crystallogr.*, 1999, **32**, 837.